J Supercond Nov Magn (2011) 24:2129–2136
DOI 10.1007/s10948-011-1166-9

ORIGINAL PAPER

Contributions from Inter-grain Boundaries to the Magneto-resistive Effect in Polycrystalline High-T_C Superconductors. The Underlying Reason of Different Behavior for YBCO and BSCCO Systems

D.A. Balaev · S.I. Popkov · S.V. Semenov · A.A. Bykov · E.I. Sabitova · A.A. Dubrovskiy · K.A. Shaikhutdinov · M.I. Petrov

Received: 4 February 2011 / Accepted: 27 March 2011 / Published online: 21 April 2011

Abstract In order to clarify the mechanisms in charge of broadening of resistive transition $R(T)$ in magnetic fields of bismuth-based polycrystalline high-T_C superconductor (HTSC), a comparative study of $Bi_{1.8}Pb_{0.3}Sr_{1.9}Ca_2Cu_3O_x$ (BSCCO) and $YBa_2Cu_3O_{7-\delta}$ (YBCO) have been performed. Magnetoresistive effects and irreversibility line obtained from magnetic measurements have been studied. It was established that (1) for YBCO, the smooth part of $R(T)$ dependence unambiguously corresponds to dissipation in the intergrain boundaries for arbitrary magnetic fields; (2) for polycrystalline BSCCO, the smooth part of $R(T)$ dependences correspond to dissipation within intergrain boundary subsystem in the field range $H < 10^2$ Oe only, while standard measurements of $R(T)$ dependences in magnetic field range $H > 10^2$ Oe reflect the dissipation processes occurring both in intergrain boundary and HTSC grain subsystems; (3) for the high-field range, the contribution from intergrain boundaries of BSCCO can be distinguished from magnetoresistance $R(H)$ dependences obtained at high enough current density on textured samples. It is proposed that various magneto-resistive properties of these classical HTSC systems are due comparatively weak pinning in BSCCO.

Keywords BSCCO · YBCO · Intergrain boundaries · Magnetoresistance

D.A. Balaev (✉) · S.I. Popkov · S.V. Semenov · A.A. Bykov · A.A. Dubrovskiy · K.A. Shaikhutdinov · M.I. Petrov
L.V. Kirensky Institute of Physics, Krasnoyarsk, 660036, Russia
e-mail: smp@iph.krasn.ru

D.A. Balaev · S.I. Popkov · E.I. Sabitova · A.A. Dubrovskiy · K.A. Shaikhutdinov
Siberian Federal University, Krasnoyarsk, 660041, Russia

1 Introduction

It is fully recognized that intergrain boundaries (IGBs) play the dominant role in the transport properties of polycrystalline HTSCs. The geometrical longitude of intergrain boundaries is of order of the superconducting coherence length. This provides Josephson-like coupling of superconducting crystallites through IGBs. So, the polycrystalline HTSCs may be considered as a "two-level" superconducting system [1]: (1) the HTSC grains and (2) network of weak links of Josephson type. Such "two-level" system manifests itself in two-step behavior of resistive transition of polycrystalline HTSCs in external magnetic field [2–8]. A typical example of $R(T)$ dependences in various magnetic fields of polycrystalline YBCO is shown in Fig. 1. The steep part of $R(T)$ broadened in high fields is associated with the resistive transition in YBCO grains while the smooth part corresponds to the superconducting transition at the IGBs [2–8]. The influence of magnetic field on the steep part of $R(T)$ has no big interest since the crystallites are randomly oriented and the effects of anisotropic magnetoresistance [9] are not seen. On the other hand, the influence of magnetic field on the smooth part of $R(T)$ dependence allows to identify the dissipation mechanisms within IGBs. The $R(T)$ dependences of polycrystalline YBCO [3, 10], La-Sr-Cu-O (LSCO) [11], and YBCO based composites [4, 12, 13] have been studied and the pinning potential in the intergrain media has been derived.

However, analysis of appropriate literature data shows that in such polycrystalline systems as Bi-, Tl-, and Hg-based HTSC compounds [14–23] the behavior of the resistive transition in a magnetic field is more complicated than that in YBCO and LSCO compounds. The origin of different behavior of $R(T)$ dependences should be disclosed. So, it is questionable—does the smooth part of $R(T)$ dependence

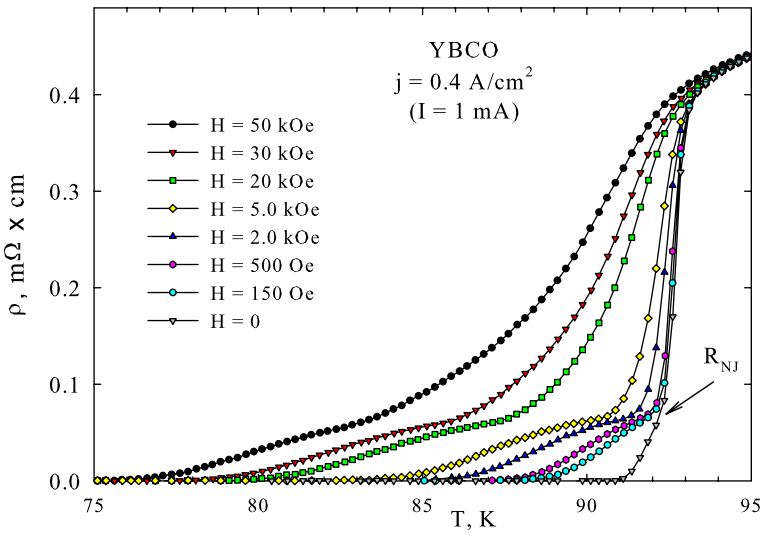

Fig. 1 The resistive transition $R(T)$ under various magnetic fields for YBCO. The maximal resistive response from IGBs is pictured as R_{NJ}

in a magnetic field correspond to the transition in IGBs or not? Isotherms of magnetoresistance $R(H)$ can exhibit peculiarities related to contributions from IGB or HTSC grain subsystems. A tendency to saturation followed by change of curvature of $R(H)$ dependence of Pr-doped YBCO allowed to distinguish the magnetic field ranges of dissipation corresponding to IGBs and superconducting grains [24]. Similar behavior was observed recently on textured Bi-based ceramic (BSCCO) [25]. In this work, we present results of detailed study of $R(H)$ data for various textured and nontextured BSCCO samples together with $R(T)$ and magnetic measurements data. Also, for the comparative analysis, YBCO ceramic was studied. We argue that in the Bi-based polycrystalline system in the high magnetic field range the dissipation takes place simultaneously in both IGB and HTSC crystallite subsystems. The reason of various behaviors of $R(T, H)$ for YBCO and BSCCO systems is discussed.

2 Experimental

Polycrystalline $YBa_2Cu_3O_{7-\delta}$ (YBCO) and $Bi_{1.8}Pb_{0.3}Sr_{1.9}Ca_2Cu_3O_x$ (hereafter denoted as poly-Bi) have been prepared by the standard solid state reaction technique. The X-ray diffraction pattern of YBCO shows only reflections from 1-2-3 structure. The analysis of X-ray diffraction pattern of poly-Bi sample reveal that the phase 2223 is dominant; a small amount of Bi2212 phase (less than 5%) was also detected.

The preparation of textured ceramics $Bi_{1.8}Pb_{0.3}Sr_{1.9}Ca_2Cu_3O_x$+Ag is described in [26]. In these textured ceramics, arranged plate-like Bi2223 crystallites have the thickness 1–2 μm and average linear dimensions 20–30 μm. The crystallographic c-axes of the crystallites are perpendicular to the surface of plates and the a–b planes are parallel to the surface. Hereafter textured samples are denoted as "text Bi/Ag30" and "text Bi/Ag0" where "30" and "0" correspond to the volume content of Ag in a sample.

The $R(T)$ and magnetoresistance $R(H)$ ($R(H) = U(H)/I$ where U is the voltage drop) dependences have been measured by the standard four-probe technique. Both PPMS (Quantum design) installation and home- made facility working in the Kirensky Institute of Physics were used. For polycrystalline YBCO and BSCCO samples, external magnetic field direction was perpendicular to the transport current density $\boldsymbol{j}$. For textured BSCCO samples, the transport current was applied along a–b planes of Bi2223 crystallites; the $\boldsymbol{H}$ direction was parallel to c-axis of Bi2223 crystallites or varied from $\boldsymbol{H} \parallel c$ to $\boldsymbol{H} \parallel a$–$b$ direction but always $\boldsymbol{H} \perp \boldsymbol{j}$. During the $R(H)$ measurements at high transport current density (the magnitude of stable transport current I up to 2.2 A), the sample was immersed in liquid nitrogen which allowed to reduce self-heating. The zero field cooled (zfc) regime was used for transport measurements.

Magnetic measurements have been performed using the vibration sample magnetometer. The specimens of cubic form $0.5 \times 0.5 \times 0.5$ mm^3 were cut from the same samples before used for transport measurements. Both zfc and field cooled (fc) regimes were used for determination of irreversibility line.

3 Results and Discussion

Figures 1 and 2 show $R(T)$ (in various external fields) and $R(H)$ (at various temperatures below T_C) dependences of studied polycrystalline YBCO.[1] The two-step shape of

[1]The authors put emphasis that the behavior seen in Fig. 1 is known for polycrystalline YBCO [3, 24] and the data obtained should be considered as typical for this system for further comparison with the BSCCO system.

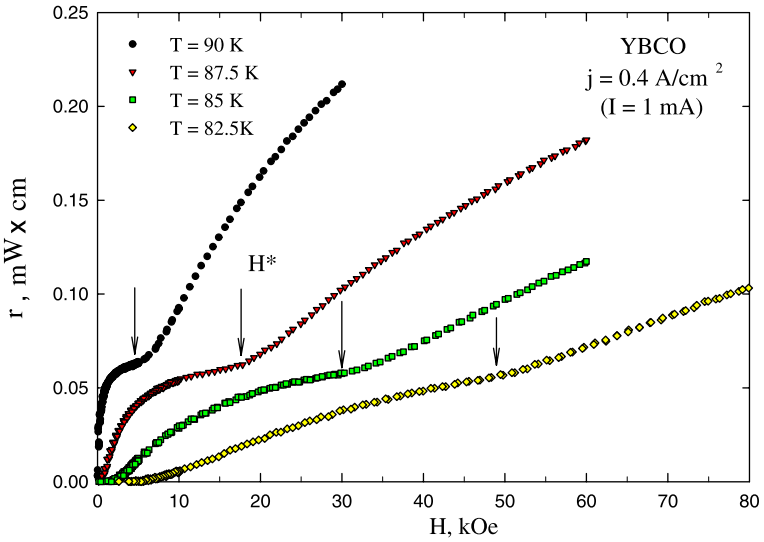

Fig. 2 Isotherms of magnetoresistance of YBCO at various temperatures. The field H^* corresponded to change of curvature of $R(H)$ dependences is pictured

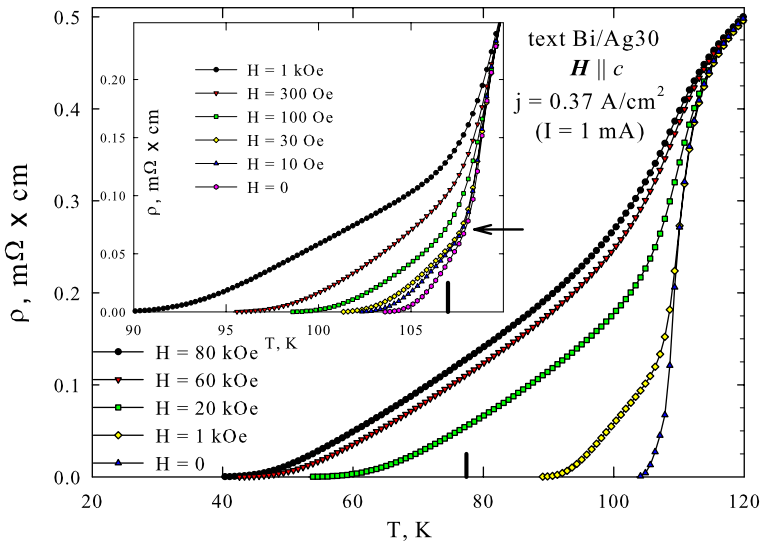

Fig. 3 The resistive transition under various magnetic fields for textured BSCCO ($\boldsymbol{H} \parallel c$ configuration). *Insert*: the same for the field range $0 \div 10^3$ Oe. The *vertical lines* indicate maximal resistive response from IGBs obtained from $R(H)$ dependences at 77.4 K (Fig. 6). *Horizontal arrow* indicates possible resistive response from IGBs for data at H lower than 10^2 Oe

$R(T)$ dependences (Fig. 1) mentioned in Introduction becomes apparent in isotherms of magnetoresistance (Fig. 2). The $R(H)$ dependences demonstrate clear plateau followed by the change of curvature at $H \approx H^*$. It is natural to assume that in the range $H \leq H^*$ the dissipation occurs at the IGBs while above H^* the dissipation takes place within the HTSC grains also. Maximal resistive response from IGBs, (the "height" of the smooth part of $R(T)$ dependence before its sharp increase) is nearly not dependent on the magnetic field. Therefore, the magnetoresistance from IGBs practically saturates before onset of dissipation within HTSC grains. The magnitude of the "height" of the smooth part of $R(T)$ dependences may be considered as the normal resistance of Josephson network R_{NJ}. The R_{NJ} value determined from $R(T)$ curves (Fig. 1) practically coincides with magnetoresistance at $H = H^*$ in Fig. 2. So, in the granular YBCO system, the dissipation processes in both IGB and HTSC crystallite subsystems are well defined. In other words, strong inequality

$$j_{\mathrm{CG}}(H) \gg j_{\mathrm{CIGB}}(H) \tag{1}$$

(where j_{CG} and j_{CIGB} are the critical current densities of HTSC grains and IGBs, respectively) retains for granular YBCO system in arbitrary magnetic fields.

Figures 3 and 4 show the $R(T)$ dependences (in various external fields) and the $R(H)$ dependences (at various temperatures below T_{C}) of the textured BSCCO sample-text Bi/Ag30. Different behavior of $R(T, H)$ dependences of YBCO and text Bi/Ag30 samples is notable. It is difficult to identify the contribution from IGBs to the $R(T)$ dependences for the sample text Bi/Ag30. There is no noticeable change of curvature of $R(T)$ dependences at high magnetic fields (20–60 kOe). Clear "two-step" shape of resistive transition is observed in magnetic fields of order $\sim 10^3$ Oe or

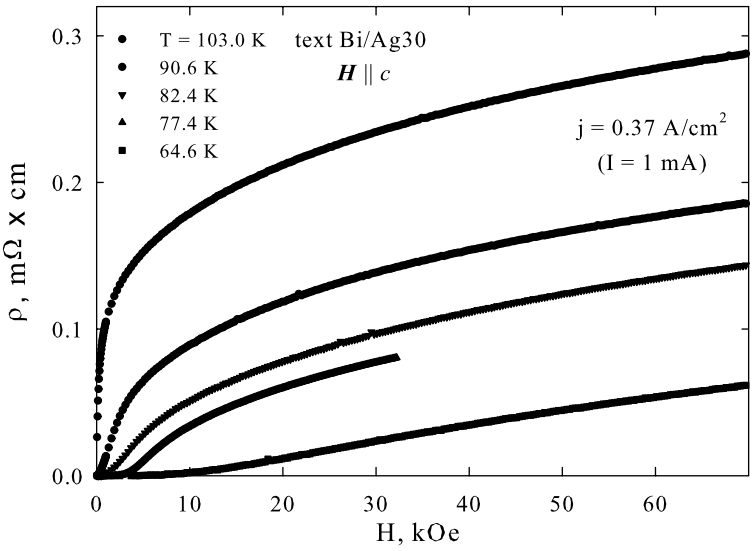

Fig. 4 Isotherms of magnetoresistance of textured BSCCO ($\boldsymbol{H} \parallel c$ configuration) at various temperatures

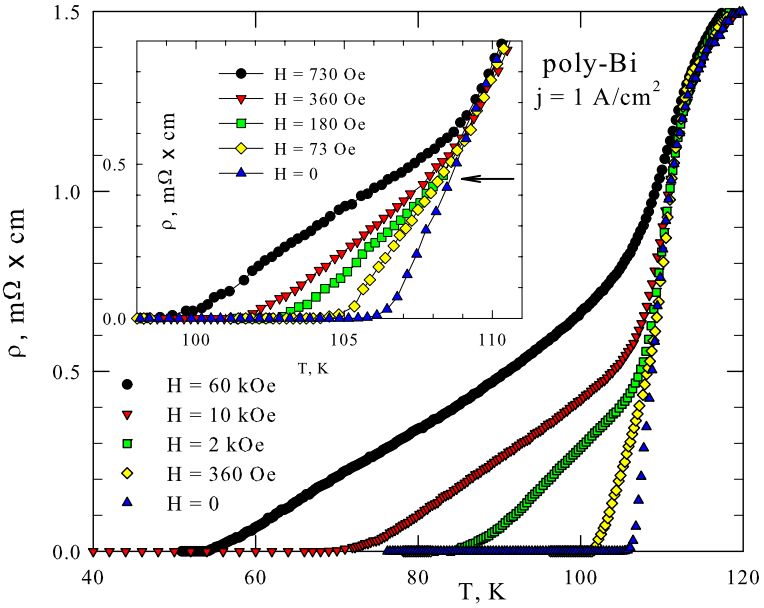

Fig. 5 The resistive transition under various magnetic fields of polycrystalline BSCCO. *Insert*: the same for the field range $0 \div 10^3$ Oe. *Horizontal arrow* indicates possible resistive response from IGBs for data at H lower than 10^2 Oe

lower. The height of resistive "tail" is nearly the same in the range $H < 10^2$ Oe while in the range $H > 10^2$ Oe it growths with increase of field. So, the R_{NJ} parameter introduced above has meaning for the weak magnetic field range only. Isotherms of magnetoresistance (Fig. 4) also do not manifest any peculiarities corresponding to saturation of magnetoresistance of subsystem of IGBs pronounced for YBCO (Fig. 2).

The nontextured BSCCO sample (poly-Bi) studied in this work demonstrates behavior of resistive transition in magnetic field (see Fig. 5) similar to sample text Bi/Ag30. Identification of contribution from IGBs is possible in the field range ($0 \div 10^2$ Oe) only.

The presence of Josephson junctions in a granular HTSC implies a strong effect of transport current on the dissipation in this subsystem. $R(T)$ and $R(H)$ dependences shown in Figs. 3 and 4 have been performed at sufficiently small current density. However, a considerable increase of transport current is problematic in measurements of $R(T)$ dependences due to Joule heat. The $R(H)$ measurements, contrariwise, may be carried out at high transport current densities when the sample is immersed in a liquid nitrogen. Figure 6 represents the $R(H)$ data for sample Text Bi/Ag30 obtained at various transport current densities ($T = 77.4$ K, $\boldsymbol{H} \parallel c$). It is clearly seen that when the transport current becomes comparable to the critical one the peculiarity on $R(H)$ dependences arises. There is a change of curvature at $H^* \approx 2$ kOe. Also, the growth of resistance with an increase of transport current is the largest in the range $H < H^*$. Such behavior, obviously, is a result of contribution from IGBs in the range

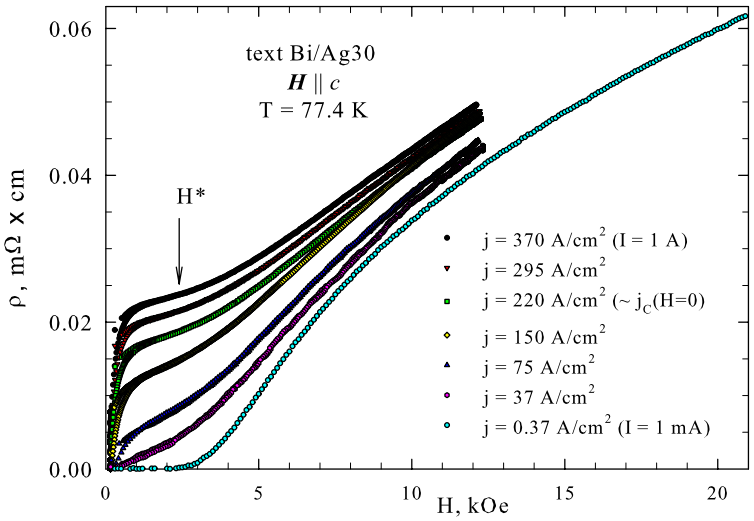

Fig. 6 The magnetoresistance of sample text Bi/Ag30 ($\boldsymbol{H} \parallel c$ configuration) at 77.4 K for various current densities (*pointed* in the figure). The field H^* corresponded to change of curvature of $R(H)$ dependences is pictured

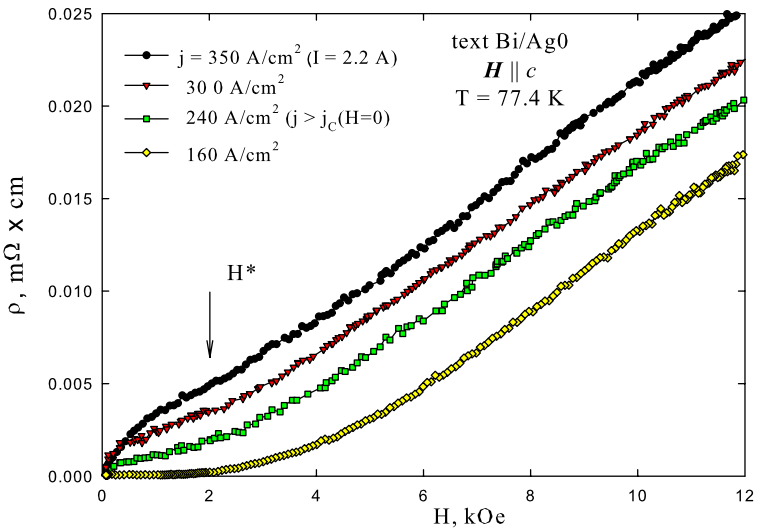

Fig. 7 The magnetoresistance $R(H)$ of sample text Bi/Ag0 ($\boldsymbol{H} \parallel c$ configuration) at 77.4 K for various current densities (*pointed* in the figure). The field H^* corresponded to change of curvature of $R(H)$ dependences is pictured

$H < 2$ kOe and onset of dissipation within BSCCO crystallites at $H^* \approx 2$ kOe. At small transport, the current appearance of magnetoresistance coincides with the onset of dissipation within BSCCO crystallites, therefore, $R(H)$ dependence at $H > 2$ kOe is caused to dissipation processes in both subsystems. The dependence $R(H) \approx 2$ kOe versus transport current has a tendency to saturation, however, total saturation of magnetoresistance from the subsystem of grain boundaries seems to achieve at higher current densities. The magnitude of $R(H) \approx 2$ kOe, $j = 370$ A/cm^2 is pointed together with $R(T)$ dependences in Fig. 3. This value is less but it is comparable to the "height" of resistive tails in weak magnetic fields.

The $R(H)$ data obtained on textured BSCCO sample without Ag (text Bi/Ag0) at various transport current densities are shown in Fig. 7. One can see from this figure that the peculiarity at $H^* \sim 2$ kOe ($\boldsymbol{H} \parallel c$) is less pronounced than for sample text Bi/Ag30 but it is also observable. So far, in the range $H < H^*$, the magnetoresistance is caused by dissipation in IGBs; one can conclude that addition of Ag results to more sensitivity of magnetoresistance of the IGB subsystem against an external magnetic field. Additionally, in the sample text Bi/Ag30, the BSCCO crystallites are ordered better than in text Bi/Ag0 (the degree of texture determined by Lotgering method is 0.97 for text Bi/Ag0 and 0.99 for text Bi/Ag30 [26]). Ordering of crystallites, possibly, gives rise to pronounced peculiarity on $R(H)$ curves (Figs. 6 and 7).

Figure 8 shows the $R(H)$ dependences of sample Text Bi/Ag30 obtained in various orientations of $\boldsymbol{H}$ and c-axis of Bi2223 crystallites.[2] The peculiarity on $R(H)$ curves

[2]The anisotropy of $R(H)$ curves seen in Fig. 8 is typical for textured ceramics and tapes [16, 27, 28]. It reflects internal anisotropy of Bi2223 crystallites although misorientation of crystallites in a sample dramatically reduces the ratio $R(\boldsymbol{H} \parallel \boldsymbol{c})/R(\boldsymbol{H} \perp c)$.

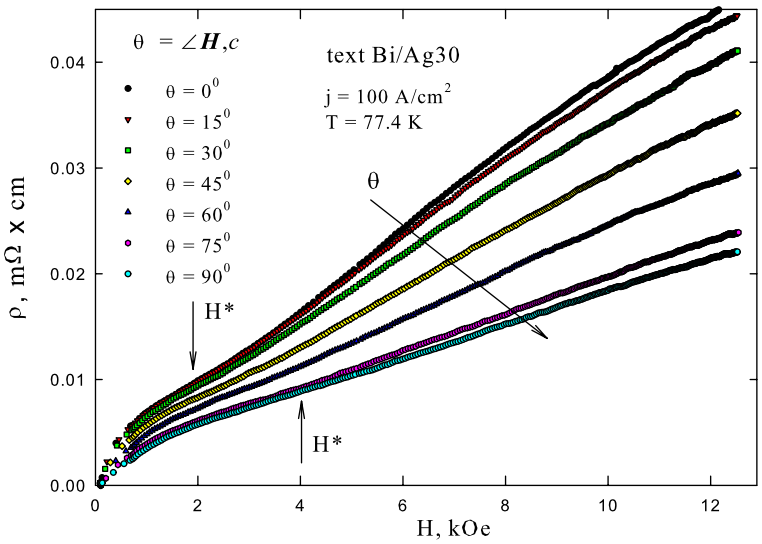

Fig. 8 The magnetoresistance of sample text Bi/Ag30 for various orientations of $\boldsymbol{H}$ and c-axis of Bi2223 crystallites. The fields H^* corresponded to change of curvature of $R(H)$ dependences for $\theta = 0°$ and $\theta = 90°$ are pictured

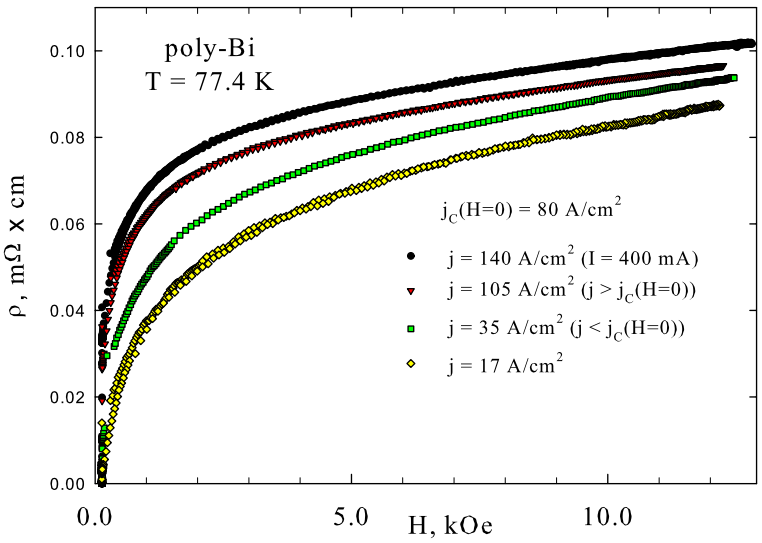

Fig. 9 The magnetoresistance of sample poly-Bi at 77.4 K for various current densities (*pointed* in the figure)

(a change of curvature) shifts to higher fields with variation of angle $\varphi = \angle \boldsymbol{H}, c$ from 0° to 90°. For $\varphi = 90°$, the peculiarity at $H = H^* \approx 4$ kOe becomes less pronounced. As a result, no peculiarities on $R(H)$ dependences are observed in nontextured polycrystalline BSCCO where there are random orientations of crystallites and angles φ. Figure 9 shows the $R(H)$ dependences of sample poly-Bi obtained at various transport current densities (the j values are both less and higher than $j_C(H = 0)$). So, for the BSCCO system, it is possible to recognize the contribution from IGBs from $R(H)$ curves on textured samples using high enough current density (at least, comparable to $j_C(H = 0)$).

It is known that the irreversibility line in H–T coordinates divides different dissipation regimes [29]. Conventional dc magnetization fc and zfc measurements may be used to find this irreversibility line [30]. We determined H_{irr}, T line from temperature dependences of dc magnetization in fc and zfc regimes. "T_{irr}" data were obtained as a point were $M_{zcf}(T)$ and $M_{fc}(T)$ at a certain field start to bifurcate. The $H_{irr}(T)$ data for samples YBCO and text Bi/Ag30 ($\boldsymbol{H} \parallel c$) are presented in Figs. 10 and 11, respectively.[3] Also, in Figs. 10 and 11, there are plotted dependences of "zero resistivity" temperature $T_{C0}(H)$ determined from $R(T)$ data in Figs. 1 and 3 by criterion 10^{-6} Ω×cm. For YBCO, the $T_{C0}(H)$ dependence is located lower than the irreversibility line in H–T coordinates. It is worth noting that if the Josephson coupling through IGBs is additionally weakened in polycrystalline YBCO the $T_{C0}(H)$ dependence shifts to the low temperature region [4, 7]. An increase of the transport current gives a similar effect [3, 7]. Above the irre-

[3] In this paper, we do not discuss details of the temperature behavior of irreversibility line of investigated samples assuming that our data is typical for these systems [29].

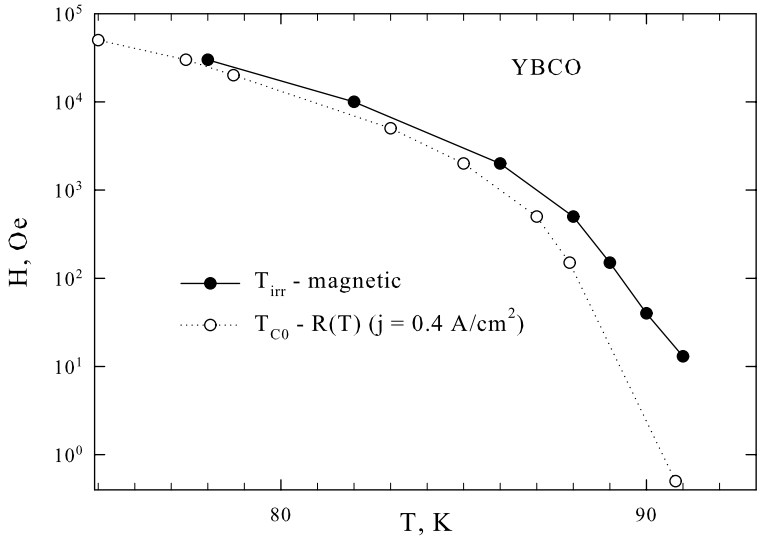

Fig. 10 The irreversibility line $H_{irr}(T)$ obtained from magnetic measurements and the dependence $T_{C0}(H)$ obtained from resistive measurements (Fig. 1) in coordinates H, T (semilog scale) for YBCO

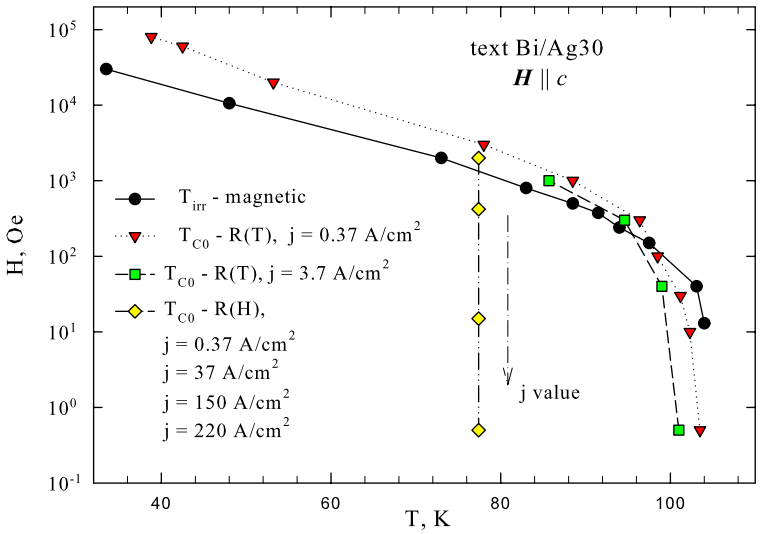

Fig. 11 The irreversibility line $H_{irr}(T)$ (obtained from magnetic measurements) and the dependences $T_{C0}(H)$ obtained from measurements of $R(T)$ and $R(H)$ at various transport currents (*pointed* in the figure) in coordinates H, T (semilog scale) of sample text Bi/Ag30. For details, see the text

versibility line, dissipation can occur in HTSC grains. For BSCCO, the $T_{C0}(H)$ dependence is located above the irreversibility line except for weak magnetic field range (lower than 10^2 Oe). Therefore, in the temperature range lower than ≈98 K (see Fig. 11), the magnetoresistance may be caused by the dissipation processes both in IGB and HTSC grain subsystems. A tenfold increase of transport current is not enough to shift $T_{C0}(H)$ lower the irreversibility line. These data are also shown in Fig. 11. If one determines the T_{C0}, H data at $T = 77.4$ K from $R(H)$ measurements (Fig. 5) assuming H is the threshold field at which $R \approx 10^{-6}$ Ω×cm, it is seen from Fig. 11 that "T_{C0}" crosses the irreversibility line with an increase of transport current. In this case, it is possible to recognize the contribution from IGBs on $R(H)$ dependences; see Fig. 5. The contribution from IGBs seems to be evident also on $R(T)$ curves at $H < 10^2$ Oe; see Fig. 3. It is clear since the temperature range of smooth parts of $R(T)$ dependences measured at $H < 10^2$ Oe (see inset in Fig. 3) is from the right of the cross-point of $H_{irr}(T)$ and $T_{C0}(H)$; see Fig. 11.

In $\boldsymbol{H} \parallel a$–$b$ geometry, the $H_{irr}(T)$ and $T_{C0}(H)$ dependences shift upward in H–T coordinates (obviously $H_{irr\parallel a-b} > H_{irr\parallel c}$, $T_{C0}(\boldsymbol{H} \parallel a\text{–}b) > T_{C0}(\boldsymbol{H} \parallel c)$, and $R(\boldsymbol{H} \parallel a\text{–}b) > R(\boldsymbol{H} \parallel c)$ [16]. Nevertheless, relative location of $H_{irr}(T)$ and $T_{C0}(H)$ dependences is nearly the same as for $\boldsymbol{H} \parallel c$ geometry. The $H_{irr}(T)$ dependence of sample text Bi/Ag0 is close to that shown in Fig. 11. A similar situation takes place for nontextured sample poly-Bi.

We regard the data obtained as typical for polycrystals of these classical HTSC systems. Therefore, the above speculations are related to granular Y- and Bi-based HTSCs. The difference of the irreversibility line of YBCO and BSCCO is mainly due to relatively weak pinning in the latter system [29]. In YBCO, inequality (1) retains for arbitrary mag-

netic fields while in BSCCO due to weak pinning inequality (1) is true only in the range $H < H_{irr}$. In this field range it is possible to reach partial saturation of magnetoresistance of the IGB subsystem by applying high enough current density (comparable to $j_C(H = 0)$). Such a behavior, however, can be observed on textured samples only. In the range $H > H_{irr}$ the dissipation processes occur simultaneously within HTSC crystallites and IGBs.

4 Concluding Remarks

Thus, difference between resistive transitions in a magnetic field of granular YBCO and BSCCO systems is caused by the following reasons. The steep and smooth parts of $R(T)$ dependence of YBCO correspond to contributions from HTSC grains and IGBs, respectively. For BSCCO, a similar situation seems to take place in the field range lower than $\sim 10^2$ Oe. In the field range above $\sim 10^2$ Oe the smooth part of $R(T)$ dependence reflect simultaneous contributions from IGBs and HTSC grains. Relatively weak pinning, and hence low irreversibility fields in BSCCO system result in dissipation to take place both within HTSC grains and IGBs. Therefore, for the range of magnetic field above $\sim 10^2$ Oe, the temperature dependence of pinning potential derived from the smooth part of $R(T)$ dependence could not be attributed to the IGBs only (for the YBCO system, this approach is entirely valid). The contribution from IGBs of the BSCCO system can be identified by measurements of magnetoresistance $R(H)$ of textured samples performed at high enough current density or from $R(T)$ dependences in weak magnetic fields.

We should generalize these conclusions to other classical HTSC systems. Really, the granular LSCO system [8, 11] exhibits clearly a two-step resistive transition in a magnetic field like YBCO. These systems are known to possess good pinning in comparison with Bi-, Tl-, and Hg-based HTSC compounds [29]. For this reason, for LSCO both contributions from superconducting crystallites and inter-crystallite boundaries are distinctively seen from $R(T)$ dependences. The effect of magnetic field on the resistive transition of Tl- and Hg-based polycrystalline HTSCs [21–23] is similar to that observed for BSCCO. So, in these granular HTSCs, the $R(T, H)$ dependences are expected to reflect magnetoresistance from both IGBs and superconducting grains. It is possible to reveal the contribution from the IGB subsystem by $R(H)$ measurements performed at a high enough current density on textured samples; so far Tl- and Hg-based HTSCs reveal high anisotropy like the BSCCO system.

Acknowledgements This work is supported by program N5 of RAS, project N7.

References

1. Ji, L., Rzchowski, M.S., Anand, N., Tinkham, M.: Phys. Rev. B **47**, 470 (1993)
2. Dubson, M.A., Herbert, S.T., Calabrese, J.J., Harris, D.C., Patton, B.R., Garland, J.C.: Phys. Rev. Lett. **60**, 1061 (1988)
3. Gaffney, C., Petersen, H., Bednar, R.: Phys. Rev. B **48**, 3388 (1993)
4. Gamchi, H.S., Russel, G.J., Taylor, K.N.R.: Phys. Rev. B **50**, 12950 (1994)
5. Joshi, R.J., Hallock, R.B., Taylor, J.A.: Phys. Rev. B **55**, 9107 (1997)
6. Daghero, D., Mazzetti, P., Stepanesku, A., Tura, P., Masoero, A.: Phys. Rev. B **66**, 184514 (2002)
7. Balaev, D.A., Shaikhutdinov, K.A., Popkov, S.I., Gokhfeld, D.M., Petrov, M.I.: Supercond. Sci. Technol. **17**, 175 (2004)
8. Balaev, D.A., Dubrovskiy, A.A., Shaikhutdinov, K.A., Popkov, S.I., Gokhfeld, D.M., Gokhfeld, Y.S., Petrov, M.I.: J. Exp. Theor. Phys. **108**, 241 (2009)
9. Palstra, T.T.M., Batlogg, B., van Dover, R.B., Schneemeyer, L.F., Waszczak, J.V.: Phys. Rev. B **41**, 6621 (1990)
10. Bhalla, G.L., Pratima: Supercond. Sci. Technol. **20**, 1120 (2007)
11. Urba, L., Acha, C., Bekeris, V.: Physica C **279**, 92 (1997)
12. Balaev, D.A., Popkov, S.I., Shaikhutdinov, K.A., Petrov, M.I.: Physica C **435**, 12 (2006)
13. Balaev, D.A., Dubrovskiy, A.A., Popkov, S.I., Shaikhutdinov, K.A., Petrov, M.I.: J. Supercond. Nov. Magn. **21**, 243 (2008)
14. Wright, A.C., Xia, T.K., Erbil, A.: Phys. Rev. B **45**, 5607 (1992)
15. Pekala, M., Bougrine, H., Lada, T., Morawski, A., Ausloos, M.: Supercond. Sci. Technol. **8**, 726 (1995)
16. Han, G.C., Ong, C.K.: Phys. Rev. B **56**, 11299 (1997)
17. Govea-Alkaide, E., Jardim, R.F., Mune, P.: Physica C **423**, 152 (2005)
18. Winton, B., Ionescu, M., Silver, T., Dou, S.X.: J. Phys. D, Appl. Phys. **38**, 2327 (2005)
19. Pu, M.H., Cao, Z.S., Wang, Q.Y., Zhao, Y.: Supercond. Sci. Technol. **19**, 462 (2006)
20. Shaikhutdinov, K.A., Balaev, D.A., Popkov, S.I., Petrov, M.I.: Supercond. Sci. Technol. **20**, 491 (2007)
21. Hettinger, J.D., Swanson, A.D., Brooks, J.C., Huang, J.Z., Chen, L.Q., Zhao, Zh.: Supercond. Sci. Technol. **1**, 349 (1989)
22. Roa-Rojas, J., Pureur, P., Mendocca-Ferreira, L., Orlando, M.T.D., Baggio-Saitovitch, E.: Supercond. Sci. Technol. **11**, 898 (2001)
23. Abou-Aly, A.I., Mostafa, M.F., Ibrahim, I.H., Awad, R., Al-Hajji, M.A.: Supercond. Sci. Technol. **15**, 938 (2002)
24. dos Santos, C.A.M., da Luz, M.S., Machado, A.J.S.: Physica C **391**, 345 (2003)
25. Balaev, D.A., Popkov, S.I., Semenov, S.I., Bykov, A.A., Shaikhutdinov, K.A., Gokhfeld, D.M., Petrov, M.I.: Physica C **470**, 61 (2010)
26. Petrov, M.I., Belozerova, I.L., Shaikhutdinov, K.A., Balaev, D.A., Dubrovskii, A.A., Popkov, S.I., Vasil'ev, A.D., Mart'yanov, O.N.: Supercond. Sci. Technol. **21**, 105019 (2008)
27. Hensel, B., Grasso, G., Flükiger, R.: Phys. Rev. B **51**, 15456 (1995)
28. Majoros, M., Glowacki, B.A., Campbell, A.M.: Supercond. Sci. Technol. **14**, 353 (2001)
29. Cohen, L.F., Jensen, H.J.: Rep. Prog. Phys. **60**, 1581 (1997)
30. Malozemoff, A.: Macroscopic magnetic properties of high temperature superconductors. In: Ginsberg, D.M. (ed.) Physical Properties of High Temperature Superconductors I, pp. 71–150. World Scientific, Singapore (1989)